

Temperature and electric field dependence of the dielectric property and domain evolution in [001]-oriented $0.34\text{Pb}(\text{In}_{1/2}\text{Nb}_{1/2})\text{O}_3-0.25\text{Pb}(\text{Mg}_{1/3}\text{Nb}_{2/3})\text{O}_3-0.41\text{PbTiO}_3$ single crystal

Y. Chen,¹ K. H. Lam,¹ D. Zhou,¹ X. S. Gao,¹ J. Y. Dai,^{1,a)} H. S. Luo,² and H. L. W. Chan¹

¹*Department of Applied Physics and Smart Materials Research Center, The Hong Kong Polytechnic University, Hong Kong, China*

²*R&D Center of Crystal, Shanghai Institute of Ceramics, Chinese Academy of Science, Jiading, Shanghai 201800, China*

(Received 26 July 2010; accepted 6 November 2010; published online 10 January 2011)

Ferroelectric domain structure and evolution, as well as phase transition, of [001]-oriented $34\text{Pb}(\text{In}_{1/2}\text{Nb}_{1/2})\text{O}_3-0.25\text{Pb}(\text{Mg}_{1/3}\text{Nb}_{2/3})\text{O}_3-0.41\text{PbTiO}_3$ single crystal has been studied through temperature and frequency-dependent relative permittivity characterization. Under dc bias, the transition temperature from rhombohedral-to-tetragonal phases becomes lower and the transition temperature from macrodomain to microdomain structures increases. Phase transition from rhombohedral to tetragonal is confirmed by temperature-dependent x-ray diffraction. These results are also well supported by direct domain observation by means of piezoresponse force microscopy under dc bias at different temperatures, as well as polarization-electric field hysteresis loop measurement. © 2011 American Institute of Physics. [doi:10.1063/1.3525163]

I. INTRODUCTION

Relaxor-based ferroelectric single crystals ($1-x$)Pb(Mg_{1/3}Nb_{2/3})O₃-xPbTiO₃ (PMN-PT) with the composition near the morphotropic phase boundary (MPB) exhibit excellent piezoelectric properties.¹⁻³ Based on their outstanding performance, devices with superior properties, such as ultrasonic motor,⁴ transducers,⁵ and actuators have been fabricated.⁶ However, the Curie temperature (T_C) is relatively low (~ 130 °C) for PMN-0.3PT⁷ and a phase transition from a ferroelectric rhombohedral (FE_r) to a ferroelectric tetragonal (FE_t) state also occurs at low temperatures (T_r about 60–85 °C).³ A rhombohedral-to-tetragonal phase transition would cause degradation of piezoelectric properties, and therefore, a low T_r transition temperature increases difficulty of fabrication process due to temperature restriction and also limits the potential in high power and high temperature applications.

To address these problems, recently, a ternary ferroelectric single crystal, Pb(In_{1/2}Nb_{1/2})O₃-Pb(Mg_{1/3}Nb_{2/3})O₃-PbTiO₃ (PIN-PMN-PT) with higher transition temperature, has been grown by the modified Bridgman method.⁸⁻¹⁰ The crystals show excellent piezoelectric and electromechanical performances. Compared to PMN-PT single crystals, the PIN-PMN-PT single crystals exhibit higher T_r and T_m (corresponding to the ferroelectric-cubic-to-paraelectric phase transition and maximum of relative permittivity).¹¹ Besides, the coercive field of the PIN-PMN-PT single crystals was also reported to be double than that of the PMN-PT single crystals.^{12,13} Therefore, the PIN-PMN-PT single crystals have a broader temperature range and higher electric field operating range for extensive applications.^{14,15}

Studies of the ferroelectric domain structure for relaxor materials have been carried out by investigating the dielectric properties with applied dc bias field on PMN-PT^{7,16-21} and PLZT.²² In those studies, transformation from macrodomain to microdomain was observed under a dc bias in the heating process. The ferroelectric domain images of PMN-PT single crystals measured and studied using piezoresponse force microscopy (PFM) has been reported.²³⁻²⁹ Besides, domain structures of the PMN-PT single crystals under electric field at different temperatures have also been extensively investigated by many researchers.²⁴⁻²⁷ However, similar studies in PIN-PMN-PT single crystals have rarely been reported.

In this work, we report the results in temperature dependence of relative permittivity and domain structure in rhombohedral 0.34PIN-0.25PMN-0.41PT (nominal composition) single crystals under different dc biases. Temperature-dependent x-ray diffraction (XRD) patterns and ferroelectric properties of this crystal are also studied.

II. EXPERIMENTAL

The [001]-oriented single crystal with a nominal composition of 0.34PIN-0.25PMN-0.41PT was grown by the modified Bridgman method in the Shanghai Institute of Ceramics. This nominal composition is very close to the rhombohedral-tetragonal MPB.³⁰ The crystalline structure of [001]-oriented single crystal was identified by an x-ray diffractometer (D8 Discover, Bruker) from 25 to 200 °C. The temperature dependence of the relative permittivity under different dc biases was measured by a LCR Meter (SR720, Stanford Research Systems) at frequencies of 100 Hz, 1 kHz, and 10 kHz. The applied dc bias field ranges from 0 to 300 V/mm in a temperature range of 25–230 °C. The temperature change rate was 2 °C/min in the heating process and –1 °C/min in the cooling process. Before every dielectric measurement,

^{a)}Electronic mail: apdaijy@inet.polyu.edu.hk.

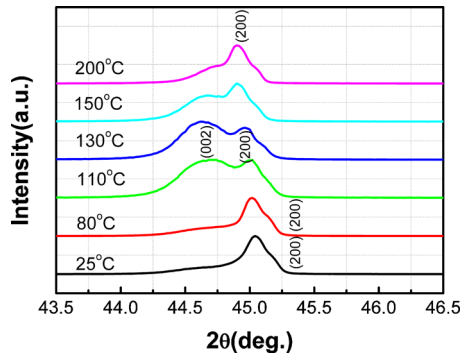


FIG. 1. (Color online) Temperature dependence of the XRD patterns of [001]-oriented PIN-PMN-PT single crystal with 2θ in the range of 43.5° – 46.5° .

the crystals were depoled. The polarization-electric field hysteresis (P – E) loops were measured using a modified Sawyer–Tower circuit at 1 Hz. Domain structures of the crystal samples were investigated using PFM (Nanoscope IV, Digital Instruments, USA).

III. RESULTS AND DISCUSSIONS

Figure 1 shows XRD patterns of the PIN-PMN-PT single crystal during heating from 25 to 200 °C. From room temperature to 80 °C, there is only one peak at about 45° corresponding to the (200) atomic plane of the perovskite structure of PIN-PMN-PT single crystal, which indicates a FE_r phase structure. At 110 °C, a split in the (002) peak

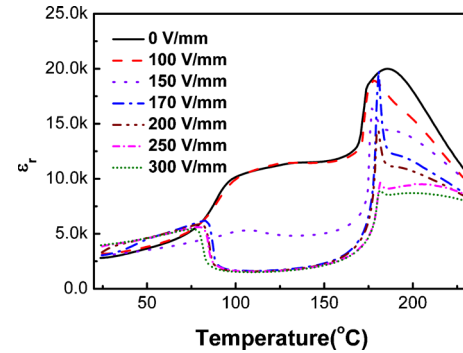


FIG. 3. (Color online) Temperature and dc bias field dependences of relative permittivity of the [001]-oriented PIN-PMN-PT single crystal at 1 kHz in heating runs.

appears at about 44.6° with the same intensity of (200) peak, suggesting a FE_t crystal structure exists at 110 °C. When temperature reaches 150 °C, the intensity of the (002) peak becomes weaker, and even disappears at 200 °C. This reveals a phase change from FE_t to paraelectric cubic phase at 200 °C. It can be concluded that the phase transition temperatures from FE_r to FE_t phases and even to paraelectric cubic phase are higher than that of PMN-PT single crystal.¹⁸

Figure 2 shows the temperature and frequency dependences of relative permittivity of the [001]-oriented PIN-PMN-PT single crystal measured with different dc bias fields during heating process. Figure 3 summarizes the temperature dependence of relative permittivity at 1 kHz as a function of

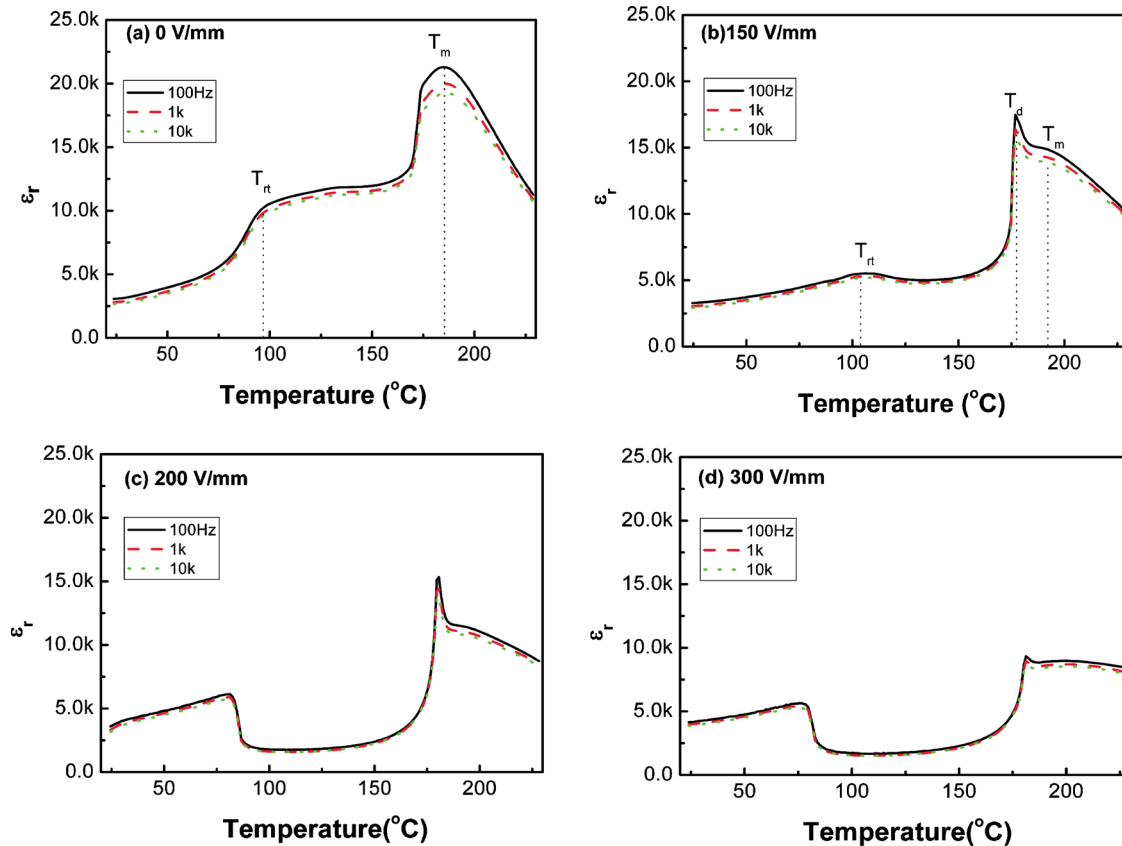


FIG. 2. (Color online) Temperature and frequency dependences of relative permittivity of the [001]-oriented PIN-PMN-PT single crystal with a dc bias field of (a) 0 V/mm, (b) 150 V/mm, (c) 200 V/mm, and (d) 300 V/mm in heating runs.

TABLE I. The temperature values of T_{rt} , T_d , and T_m in the heating and cooling processes.

E_{dc} (V/mm)	Heating process (°C)			Cooling process (°C)		
	T_{rt}	T_d	T_m	T_{rt}	T_d	T_m
0	97	...	186	72	...	180
100	98	177	190	65	...	182
150	105	177	190	59	...	184
170	83	180	194	58	...	189
200	81	180	194	58	...	194
250	80	181	205	56	...	204
300	77	181	205	56	...	204

dc bias field upon heating. From these results, it can be seen that at zero bias there is a shoulder (T_{rt}) at about 100 °C which is corresponding to the rhombohedral-to-tetragonal phase transition.¹⁸ T_m can be determined to be 186 °C from the heating process, and frequency dispersion behavior can be clearly seen. However, one can see that when the dc bias increases to 150 V/mm, frequency dispersion in the relative permittivity almost disappears and the dielectric-temperature curve shoulder T_{rt} changes to a small peak. When the bias further increases to 170 V/mm, the peak of T_{rt} is very sharp, and the rhombohedral-to-tetragonal phase transition temperature is significantly lowered. The rhombohedral-to-tetragonal phase transition temperature further decreases as the dc bias further increases. This suggests that the tetragonal macro-

domain becomes predominant when a dc bias is applied on the [001]-oriented crystal.⁷ The applied dc bias along [001] should stabilize the FE_t macrodomain phase, whose polar direction is along the [001] orientation. Besides, the frequency dispersion behavior becomes weaker between T_{rt} and T_m . In addition, one can also see from Figs. 2 and 3 that, there is a sharp temperature T_d , which corresponds to the evolution of macrodomain to microdomain state in the heating process.²¹ Table I shows the temperature values of T_{rt} , T_d , and T_m . The added dc bias makes this conversion confined in a more narrow temperature range with a sharp increase in relative permittivity when a dc bias is applied.

Temperature and frequency dependence of relative permittivity in the [001]-oriented PIN-PMN-PT single crystal measured with different dc bias fields upon cooling are shown in Fig. 4. Figure 5 summaries the temperature dependence of the relative permittivity at 1 kHz as a function of dc bias field in cooling runs. Compared to the heating process, the two characteristic dielectric peaks at T_{rt} and T_m are still visible [except for Fig. 4(b)]. Similar to that during the heating process, the T_m peak shifts to higher temperature with dc bias increasing, and as a result the temperature range between T_{rt} and T_m becomes broader. This phenomenon suggests that the tetragonal phase of the PIN-PMN-PT single crystal can be induced at lower temperature under dc bias conditions.

However, it is apparent that there is a large dielectric hysteresis when temperature sweeps from heating and cooling, suggesting that the phase transition process is thermody-

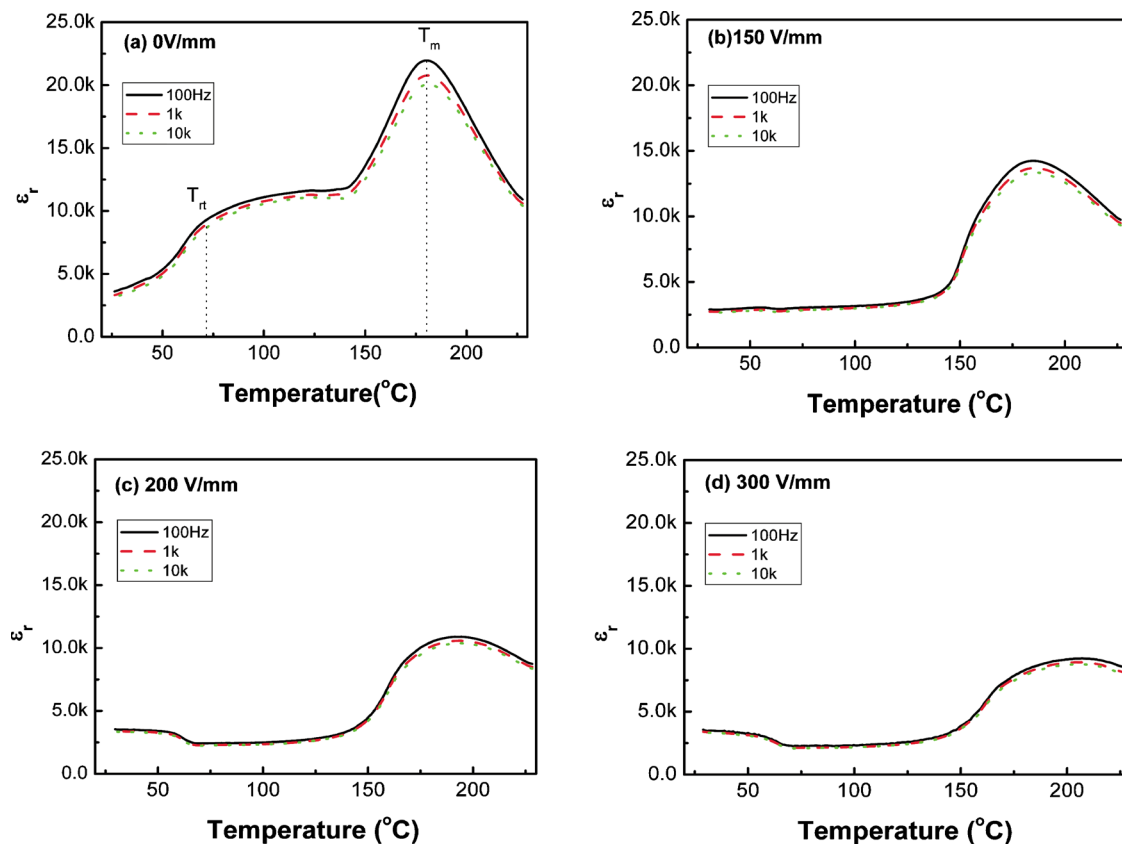


FIG. 4. (Color online) Temperature and frequency dependence of relative permittivity of the [001]-oriented PIN-PMN-PT single crystal with a dc bias field of (a) 0 V/mm, (b) 150 V/mm, (c) 200 V/mm, and (d) 300 V/mm in cooling runs.

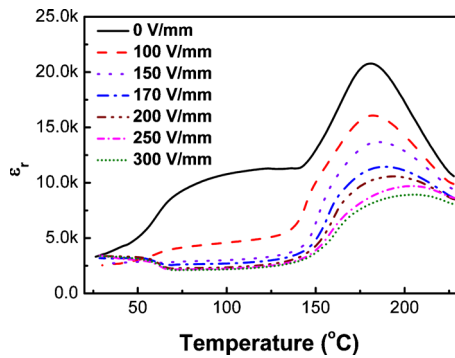


FIG. 5. (Color online) Temperature and dc bias field dependence of relative permittivity of the [001]-oriented PIN-PMN-PT single crystal at 1 kHz in cooling runs.

namically irreversible.¹⁶ Some distinct differences can be found between the temperature-dependent relative permittivity curves during heating and cooling processes under bias. The most significant difference is that the T_m peak in the cooling run is suppressed and the macrodomain-to-microdomain transition temperature T_d can hardly be identified in the cooling process either with or without bias. Besides, the temperature values corresponding to the phase transition in cooling process were given in Table I. We can understand this by the fact that during heating, tetragonal macrodomains change to microdomains by breaking larger domains into smaller domains accompanied by generation of large amount of domain walls; while these domain walls movement contributes to the dielectric constant significantly. But during the cooling process under electric field, small domains merged into larger domains by reducing the number of domain walls; therefore, there are less movement of domain walls and thus results in a suppressed dielectric constant.

In order to understand the temperature-dependent relative permittivity during phase transition, temperature-dependent P - E hysteresis loops have been measured as shown in Fig. 6, where it can be seen that at room temperature, the remnant polarization P_r is $31 \mu\text{C}/\text{cm}^2$ and the coercive field E_c is $0.3 \text{ kV}/\text{mm}$. During heating from 80 to 110°C , which corresponds to the rhombohedral-to-tetragonal phase transition temperature, P_r value increases to $33 \mu\text{C}/\text{cm}^2$. This indicates that P_r of tetragonal phase is larger than that of rhombohedral phase. The increase in the remnant polarization P_r is accompanied by a decrease in the

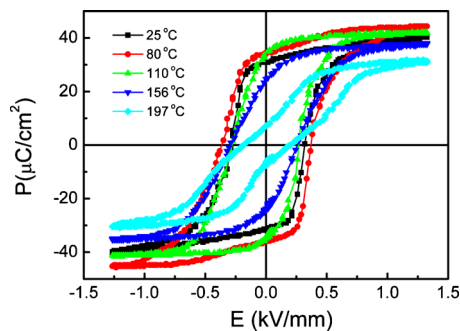


FIG. 6. (Color online) Temperature dependence of P - E hysteresis loops of the [001]-oriented PIN-PMN-PT single crystal.

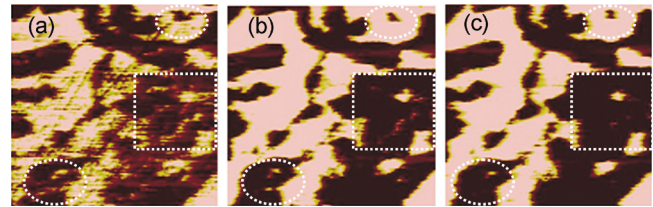


FIG. 7. (Color online) PFM images of the PIN-PMN-PT single crystal upon heating to (a) 55°C , (b) 83°C , and (c) 100°C , scan size: $2.4 \times 2.4 \mu\text{m}^2$.

relative permittivity. The decrease in relative permittivity may be understood by the fact that the formation of tetragonal phase increases the dimension along the electric field which is the [001] direction of the crystal and therefore results in a decrease in capacitance. A sharp decrease in P_r is observed at 156°C at which the macrodomain state changes to microdomain state. This transition results in a sharp peak in the relative permittivity, contributed by large movement of domains walls. When temperature increases to 197°C (beyond T_m), the P_r drops significantly, indicating the phase transition from FE_t to PE_c , and corresponds to further decrease in relative permittivity due to the formation of paraelectric phase.

Temperature-dependent ferroelectric domain structure and evolution under dc bias was also studied. Figure 7 shows the PFM domain images of the PIN-PMN-PT single crystal at 55°C , 83°C , and 100°C without applying a bias voltage, respectively. From 55 to 100°C , there is no significant change in the observed domain structure.²⁶ However, the sizes of domains, for example, a black speckle and white spots (in zones), change and they even disappear when temperature increases. The gradual domain growth and vanish of some small domains are due to the rhombohedral-to-tetragonal phase transition.

Figure 8 shows PFM images of PIN-PMN-PT single crystal with and without a dc bias at 25°C and 100°C , respectively. At low temperature (25°C), the dc bias causes domain switching indicated by domain size increase; while the domain contrast also becomes sharper as shown in Figs. 8(a) and 8(b). However, an apparent change occurs in the domains subjected to an electric field when the temperature

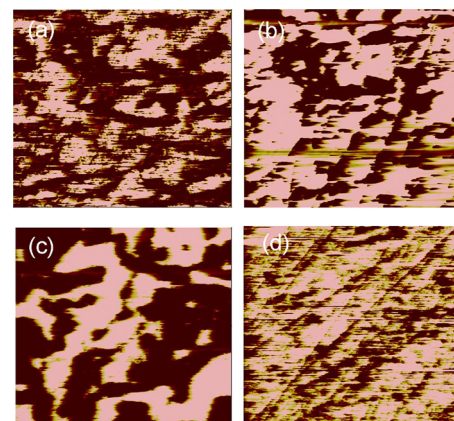


FIG. 8. (Color online) PFM images (left column: without dc bias; right column: under $170 \text{ V}/\text{mm}$ dc bias) of the PIN-PMN-PT single crystal at (a) and (b) 25°C and (c) and (d) 100°C , scan size: $5 \times 5 \mu\text{m}^2$.

is high [100 °C as shown in Fig. 8(d)], where almost all domains switch to one orientation (formation of single domain) under 170 V/mm dc bias except for some dark spots, which may be due to the defect pinning or the nature of relaxor ferroelectrics (nanodomains always exist).²⁶ The formation of larger macrodomain, also the phase transition from rhombohedral to tetragonal, matches the fact that there is a relative permittivity decrease in the temperature-dependent dielectric curve under dc bias.

IV. CONCLUSIONS

The temperature and dc bias-dependent dielectric and ferroelectric properties of the PIN-PMN-PT single crystal, as well as ferroelectric domain structure and evolution, have been studied. It is found that, upon heating, the crystal transforms from FE_r phase to FE_t phase and then to PE_c phase. The dielectric characteristics of the crystal show that the FE_t phase at temperatures between T_{rt} and T_d can be reinforced by applying dc bias along the [001] direction. The P - E hysteresis at increased temperatures reveals that, the transformation to the FE_t phase is accompanied by a P_r increment until T_d . These conclusions are supported by the PFM observations.

ACKNOWLEDGMENTS

This work was supported by the Hong Kong Innovative Technology Council (Project No. ITS/044/09 FP) and the Centre for Smart Materials of the Hong Kong Polytechnic University.

¹S. E. Park and T. R. Shrout, *J. Appl. Phys.* **82**, 1804 (1997).

²R. F. Service, *Science* **275**, 1878 (1997).

³D. Zhou, F. Wang, L. Luo, J. Chen, W. Ge, X. Zhao, and H. Luo, *J. Phys. D: Appl. Phys.* **41**, 185402 (2008).

⁴L. Luo, H. Zhu, C. Zhao, H. Wang, and H. Luo, *Appl. Phys. Lett.* **90**, 052904 (2007).

⁵D. Zhou, J. Chen, L. Luo, X. Zhao, and H. Luo, *Appl. Phys. Lett.* **93**, 073502 (2008).

⁶Z. Feng, T. He, H. Xu, H. Luo, and Z. Yin, *Solid State Commun.* **130**, 557

(2004).

⁷X. Zhao, J. Wang, H. L. W. Chan, C. L. Choy, and H. Luo, *Appl. Phys. A: Mater. Sci. Process.* **80**, 653 (2005).

⁸Y. P. Guo, H. S. Luo, T. H. He, and Z. W. Yin, *Solid State Commun.* **123**, 417 (2002).

⁹J. Tian, P. D. Han, X. L. Huang, H. X. Pan, J. F. Carroll, and D. A. Payne, *Appl. Phys. Lett.* **91**, 222903 (2007).

¹⁰G. S. Xu, K. Chen, D. F. Yang, and J. B. Li, *Appl. Phys. Lett.* **90**, 032901 (2007).

¹¹X. Z. Liu, S. J. Zhang, J. Luo, T. R. Shrout, and W. W. Cao, *J. Appl. Phys.* **106**, 074112 (2009).

¹²J. Luo, W. Hackenberger, S. J. Zhang, and T. R. Shrout, in Proceedings of the 2008 IEEE International Ultrasonics Symposium (IUS), Beijing, China, November 2–5 2008, pp.261–264.

¹³P. Sun, Q. F. Zhou, B. P. Zhu, D. W. Wu, C. H. Hu, J. M. Cannata, J. Tian, P. D. Han, G. F. Wang, and K. K. Shung, *IEEE Trans. Ultrason. Ferroelectr. Freq. Control* **56**, 622 (2009).

¹⁴P. Yu, F. F. Wang, D. Zhou, W. W. Ge, X. Y. Zhao, H. S. Luo, J. L. Sun, X. J. Meng, and J. H. Chu, *Appl. Phys. Lett.* **92**, 252907 (2008).

¹⁵S. J. Zhang, J. Luo, W. Hackenberger, and T. R. Shrout, *J. Appl. Phys.* **104**, 064106 (2008).

¹⁶Z. R. Li, Z. Xu, X. Yao, and Z. Y. Cheng, *J. Appl. Phys.* **104**, 024112 (2008).

¹⁷Z. R. Li, Z. Z. Xi, Z. Xu, and X. Yao, *J. Mater. Sci. Lett.* **21**, 1325 (2002).

¹⁸X. Y. Zhao, J. Wang, H. L. W. Chan, C. L. Choy, and H. S. Luo, *J. Phys.: Condens. Matter* **15**, 6899 (2003).

¹⁹X. Y. Zhao, J. Wang, Z. Peng, K. H. Chew, H. L. W. Chan, C. L. Choy, and H. S. Luo, *Physica B* **339**, 68 (2003).

²⁰Z. Y. Feng, X. Y. Zhao, and H. S. Luo, *J. Phys.: Condens. Matter* **16**, 3769 (2004).

²¹X. Y. Zhao, J. Wang, Z. Peng, H. L. W. Chan, C. L. Choy, and H. S. Luo, *Mater. Res. Bull.* **39**, 223 (2004).

²²X. Yao, Z. L. Chen, and L. E. Cross, *J. Appl. Phys.* **54**, 3399 (1983).

²³H. Okino, T. Ida, H. Ebihara, H. Yamada, K. Matsushige, and T. Yamamoto, *Jpn. J. Appl. Phys., Part 1* **40**, 5828 (2001).

²⁴V. V. Shvartsman and A. L. Kholkin, *Phys. Rev. B* **69**, 014102 (2004).

²⁵X. Zhao, J. Y. Dai, J. Wang, H. L. W. Chan, C. L. Choy, X. M. Wan, and H. S. Luo, *Phys. Rev. B* **72**, 064114 (2005).

²⁶K. S. Wong, J. Y. Dai, X. Y. Zhao, and H. S. Luo, *Appl. Phys. Lett.* **90**, 162907 (2007).

²⁷X. Zhao, J. Y. Dai, J. Wang, H. L. W. Chan, C. L. Choy, X. M. Wan, and H. S. Luo, *J. Appl. Phys.* **97**, 094107 (2005).

²⁸H. Okino, T. Ida, H. Ebihara, and T. Yamamoto, *Ferroelectrics* **268**, 119 (2002).

²⁹F. Bai, J. Li, and D. Viehland, *Appl. Phys. Lett.* **85**, 2313 (2004).

³⁰D. B. Lin, Z. R. Li, F. Li, Z. Xu, and X. Yao, *J. Alloys Compd.* **489**, 115 (2010).